Earth and Planetary Science Letters, 104 (1991) 424–439
Elsevier Science Publishers B.V., Amsterdam

[DT]

Cosmic ray labeling of erosion surfaces: *in situ* nuclide production rates and erosion models

D. Lal

Scripps Institution of Oceanography, Geological Research Division, University of California, 9500 Gilman Drive, La Jolla, CA 92093, USA

Received April 22, 1990; revision accepted December 10, 1990

ABSTRACT

A number of *in situ* cosmogenic radionuclides and stable nuclides have been measured in natural exposed rock surfaces with a view to study their *in situ* production and rock erosion rates [1]. The *in situ* radionuclides can be used for a high-resolution tomography of the erosional history of an exposed surface; two stable nuclides (^{3}He, ^{21}Ne) and five radionuclides (^{10}Be, ^{26}Al, ^{36}Cl, ^{14}C, ^{39}Ar) having half-lives in the range of ~ 300–1.5×10^{6} yr half-life are measurable in many rock types.

A prerequisite for the application of the *in situ* nuclides for the study of erosional histories of surfaces is a knowledge of their production rates under different irradiation conditions; altitude, latitude, irradiation geometry and shielding. Relative nuclide production rates can be determined fairly accurately using the extensive available data on cosmic ray neutrons [2]. Absolute nuclide production rates cannot generally be predicted with any accuracy because of lack of data on excitation functions of nuclides unless some normalization is possible, as was done in the case of several cosmic ray produced isotopes in the atmosphere [3]. Based on a recent natural calibration experiment in which erosion free surfaces exposed to cosmic radiation for $\sim 11{,}000$ yrs were sampled, the absolute production rates of ^{10}Be and ^{26}Al in quartz have been accurately estimated for mountain altitudes in Sierra Nevada [4]. The absolute production rates of ^{10}Be and ^{26}Al in quartz can therefore be estimated fairly accurately for any given latitude and altitude. Some measurements of ^{14}C in rocks of low erosion rate [5] similarly allow an estimate of its production rate. Attempts made to measure the *in situ* production rates of ^{3}He in rocks have not yet led to a convergent production rate. In view of the importance of knowing the production rates of isotopes of He, Ne and Ar, I present here theoretical estimates of their production rates based on available cross-section data.

I discuss the information that can be extracted from the study of the *in situ* nuclides in rocks. Useful parameters characterizing the exposure history of a rock surface are: (1) the effective surface exposure age; and (2) the time-averaged erosion rate. The implications of these parameters for single and multiple nuclide studies are discussed in terms of the erosion models considered.

1. Introduction

An important recent contribution to geomorphology has been the development of a nuclear method applicable for the study of erosion and sedimentation rates, and surface exposure ages [8–11]. The basis of the method is the *in situ* production of nuclides in solids by particles of the cosmic radiation. Note that to date, studies of cosmic-ray produced isotopes on the earth have largely been confined to those isotopes which are produced in the earth's atmosphere. Cosmic ray intensity is appreciably reduced at mountain altitudes due to nuclear interactions making it hard to detect the *in situ* produced nuclides. Until recently, it has not been possible to study the *in situ* cosmogenic radionuclides although their production and usefulness had been discussed earlier [2,12,13]. The recent advances in isotope measurement techniques, in particular the accelerator mass spectrometry (AMS) now makes it possible to detect these isotopes. To date, nine radionuclides of half-lives between 35 days and 1.5 m.y., and three stable nuclides thus produced have been detected [1]. The first application of the *in situ* produced ^{10}Be and ^{26}Al radionuclides to the study of erosion of exposed rock surfaces was made by Nishiizumi et al. [14] although these nuclides were detected earlier by Yiou et al. [15] in terrestrial impact glasses. Measurements of *in situ* cosmo-

0012-821X/91/$03.50

genic ^{3}He were made [9,10] to determine rock erosion rates. Phillips et al. [11,16] studied *in situ* produced ^{36}Cl for exposure dating of rock surfaces. Since then extensive studies have been made of ^{10}Be and ^{26}Al to determine rates of erosion of a large number of exposed surfaces [17,18]. These data have successfully demonstrated the potential of the nuclear method in geomorphology.

A prerequisite for the application of the *in situ* nuclides for the study of erosional histories of surfaces is a knowledge of their production rates under different irradiation conditions; altitude, latitude, irradiation geometry and shielding. I show that it is sufficient to obtain the production rate of a nuclide in the target of interest at any one location; production rates at other sites can be obtained accurately using the cosmic ray neutron data. Direct measurements of production rates based on studies of rocks of known exposure histories are available for ^{10}Be, ^{26}Al and ^{14}C in quartz [4,5]. Similar data are also available for ^{3}He and ^{36}Cl [6,7,16,19].

In this paper, I present latitude–altitude production rates for ^{10}Be, ^{26}Al and ^{14}C in quartz based on direct measurements of their production rates; I also give (approximate) theoretically estimated production rates for isotopes of He, Ne and Ar in different target materials, based on the available excitation functions. The second part of this paper deals with erosion models which can be used with single and multiple nuclides. The models highlight the type of geomorphological information which can be extracted using *in situ* nuclides, and also underscores the importance of knowing the nuclide production rates accurately.

2. Nuclide production rates at (0–10) km altitudes

The fluxes and energy spectra of nuclear interacting particles in the atmosphere were derived earlier [2] for estimating atmospheric production rates of nuclides. Three principal mechanisms for the production of the nuclides are: (a) by high energy spallation of nucleons (of kinetic energy, $E > 40$ MeV); (b) by thermal neutron capture reactions; and (c) by muon induced nuclear disintegrations (including capture of negative muons and coulombic interactions of fast muons). In the case of high-energy spallations, protons and alpha particles contribute less than 10%; photons are an order of magnitude less significant. Muon reactions become important only at depths below sea level [2,20].

Accurate estimations of production rates are generally not possible because of lack of knowledge of the probabilities of formation of nuclides in the different reactions. Neutron excitation functions as well as data for relevant nuclides in negative muon capture are also not available for most of the reactions of interest. In order to circumvent this problem, Lal et al. [3] determined production rates of several nuclides in Ar and O by exposing them to cosmic ray particles. Subsequent studies extended these studies to ^{22}Na and ^{28}Mg in Ar [21] and to ^{22}Na and ^{24}Na in Al and Mg [13].

2.1. *^{10}Be and ^{26}Al production in quartz*

In the case of ^{10}Be and ^{26}Al, their activities have been measured in quartz [4] extracted from "zero" erosion surfaces exposed at altitudes of 2–3.5 km, at geomagnetic latitude 44°N, for ~ 11,000 yrs in the Sierra Nevada ranges. Glacially polished surfaces studied ensured that the exposed surface did not erode during exposure and also that prior to the last exposure they were well shielded from cosmic radiation. ^{10}Be and ^{26}Al are produced in nuclear spallations of O and Si, and also by negative muon capture reactions with O and Si. Fortunately, their relative yields in muon capture, based on studies of artificially accelerated negative muons [4] are known. Basing on the published negative muon capture rates in the atmosphere, Nishiizumi et al. [4] were able to separately determine the ^{10}Be and ^{26}Al production rates in quartz due to fast nucleons and negative muons. Since the energy spectrum of nucleons of energy < 400 MeV (responsible for $> 80\%$ of nuclide production in spallation reactions) becomes invariant [2] at atmospheric depths exceeding 200 gm cm^{-2} (altitude < 12 km), the spallation yields of ^{10}Be and ^{26}Al in nuclear disintegrations are also invariant in the altitude interval 0–12 km above sea level. The absolute production rates of ^{10}Be and ^{26}Al at all latitudes and altitudes (0–12) km can therefore be determined, basing on the relative variation in the total disintegration rates in the atmosphere [2]. Likewise, one can also determine the production rates of ^{10}Be and ^{26}Al due to negative muon capture rates at all latitude and al-

titudes, since the variation in the capture rate of negative mu-mesons in the atmosphere is fairly well known [1] for atmospheric depths exceeding 200 g cm^{-2}.

The neutron data used by Lal and Peters [2] refer to the period 1948–1949, a period of higher than average solar activity. Taking into account the temporal variations in the primary cosmic ray flux with changes in the solar activity and in the neutron flux at different latitudes/altitudes, they estimated that during an average solar cycle (based on observed sun spots in 19 solar cycles), the mean global nuclear disintegration rate in the atmosphere would be higher by 4% than in 1948–49. The corresponding latitude averaged temporal variations in nuclear disintegration rates within the troposphere would of course be much smaller; the exact variation can be deduced for different altitudes/latitudes for any specified change in the primary flux or in the solar activity using the procedures discussed earlier [2].

Besides Lal and Peters [2], two other calculations have been reported by Yokoyama et al. [13] and O'Brien [22]. We adopted the latitude–altitude curves of Lal and Peters [2] because they are based on experimentally measured fluxes of slow neutrons in the atmosphere. The extensive cosmic ray data allow obtaining flux of low- and high-energy neutrons at all altitudes and latitudes in the atmosphere; in fact the relative fluxes are over-determined by the available data, and permit an internal check on the different experimental data [23]. Within the troposphere these data directly give the latitude–altitude variation for nuclear disintegrations produced by nucleons of energy < 400 MeV. Those due to higher energy particles, contributing less than 20%, can easily be calculated basing on studies of nuclear disintegrations in nuclear emulsions and cloud chambers [23]. These corrections have been made and the relative variations in all nuclear disintegrations due to nucleons of $E > 40$ MeV has been determined [2,23]. The calculations of Yokoyama et al. [13] and O'Brien [22] are on the other hand, based on nuclear cascade models. The atmosphere is equivalent to a thickness of ~ 12 nuclear interaction mean free paths, and even a 10% error in one of the nucleonic cascade parameters if linear, can lead to a ca. 120% error in flux at sea level. It should be noted that there do exist substantial disagreements between the three latitude–altitude curves [2,13,22], which is not unexpected. However, we have sufficient confidence in the curves given by Lal and Peters [2] since they are primarily based on experimentally determined neutron fluxes. The relative latitude–altitude variation in nuclear disintegrations should be accurate within $\pm 10\%$.

Scaling the measured ^{10}Be and ^{26}Al production rates in quartz in Sierra Nevada rock samples [4], I have estimated total production rates of ^{10}Be and ^{26}Al in quartz at different latitudes and altitudes. The production rate, $q(L, y)$ at geomagnetic latitude, L and altitude, y (km), can be well represented in terms of a third degree polynomial:

$$q(L, y) = a(L) + b(L)y + c(L)y^2 + d(L)y^3 \quad (1)$$

TABLE 1

Production rates * of ^{10}Be and ^{26}Al in quartz (g^{-1} SiO_2 yr^{-1})

Geomagnetic latitude	Polynomial coefficients							
	a		b		c		d	
	^{10}Be	^{26}Al	^{10}Be	^{26}Al	^{10}Be	^{26}Al	^{10}Be	^{26}Al
0°	3.511	21.47	2.547	15.45	0.95125	5.751	0.18608	1.1154
10°	3.360	22.0	2.522	15.32	1.0668	6.444	0.18830	1.1287
20°	4.0607	24.84	2.734	16.61	1.2673	7.652	0.22529	0.3504
30°	4.994	30.55	3.904	23.67	0.9739	5.911	0.42671	2.5563
40°	5.594	34.21	4.946	29.92	1.3817	8.361	0.53176	3.1853
50°	6.064	37.08	5.715	34.57	1.6473	9.955	0.68684	4.1138
60–90°	5.994	36.67	6.018	36.38	1.7045	10.30	0.71184	4.2634

* Total production rates (due to nucleons and muons) at different latitudes are given by a third-degree polynomial in altitude, y in km (eqn. 1). The polynomials are valid for 0–10 km altitudes.

where the coefficients a, b, c and d are functions of L. The best fit values of the coefficients are given in Table 1 for 0–90° geomagnetic latitudes, and 0–10 km altitudes.

The experimental uncertainties in production estimates are ±5% and ±7.5% for ^{10}Be and ^{26}Al respectively. The ^{10}Be/^{26}Al ratio at production is known within ±7%. However the absolute production rates of ^{10}Be and ^{26}Al may be uncertain due to our lack of knowledge of the exact age of the Tioga glaciation, and of secular variations in the earth's geomagnetic field. The latter is estimated to contribute an uncertainty of < 10%. For details see Nishiizumi et al. [4].

2.2. *^{14}C production in quartz*

The concentration of *in situ* ^{14}C was measured [6] in a quartzite surface sample from Allan Hills (altitude = 2000 m; geomagnetic latitude ~ 60°N) to be $(8.2 \pm 1) \times 10^5$ atoms/g. Based on studies of *in situ* ^{10}Be and ^{26}Al in this sample [18], the ^{14}C activity is expected to be in secular equilibrium with production, corresponding to a production rate of 99 ± 12 atoms ^{14}C/(g quartz yr). The relative ^{14}C:^{10}Be production rates are found to be 3.25 : 1, since the total production rate of ^{10}Be at the Allan Hill site is estimated to be 30.5 atoms/(g quartz year).

Considering the threshold energy required for the formation of ^{14}C in spallations of oxygen and silicon, and also considering that some ^{14}C is also produced in the capture of negative muon by oxygen, we deduce that the relative variation in the production rate of ^{14}C from quartz in the troposphere is best described by the variations in nuclear disintegration rates in the atmosphere.

For convenience, we give below a third-degree polynomial fit as in equation (1) for the total rate of nuclear disintegrations, s, (/gm yr) in air due to nucleons of energy $E > 40$ MeV, given by Lal and Peters [2] as a function of atmospheric pressure. The coefficients of the nuclear disintegration polynomial for 0–90° geomagnetic latitudes and 0–10 km are given in Table 2. To convert altitude, y (km), to pressure, P (g cm^{-2}) I used the ICAO standard atmosphere [24]; the data are well represented (within 0.03% for 0–6 km and within 0.5% for 6–10 km) by a polynomial $P = p1 + p2 \cdot y + p3 \cdot y^2 + p4 \cdot y^3$ with $p1 = 1032.92$, $p2 = -121.95$, $p3 = 5.657$ and $p4 = -0.1095$.

The production rate of ^{14}C in quartz at any latitude/altitude is obtained by multiplying the total nuclear disintegration rate in the atmosphere at that site by 3.1×10^{-2}.

2.3. *Production rates of ^{3}He, ^{20}Ne, ^{21}Ne, ^{22}Ne, ^{36}Ar and ^{38}Ar*

The production rates of ^{3}He have been measured in plagioclases and pyroxenes from studies of rocks of constrained exposure histories [6,7]. I will summarize here the available production estimates for ^{3}He in olivine phenocrysts. Kurz et al. [6] studied Hawaiian lava flows and obtained mean values of 187 ± 45, 82 ± 22 and 190 ± 28 ^{3}He atoms/(g yr) during 0–2000, 2000–7000 and 7000–10,000 yr BP, respectively, at sea level and high latitudes (≥ 60); I have scaled their values for sea level at Hawaii by a factor of 1.5. The

TABLE 2

Nuclear disintegration rates * in the atmosphere (g^{-1} yr^{-1})

Geomagnetic latitude (°)	Polynomial coefficients			
	$a1$	$a2$	$a3$	$a4$
0	3.307×10^2	2.559×10^2	9.843×10^1	2.050×10^1
10	3.379×10^2	2.521×10^2	1.110×10^2	2.073×10^1
20	3.821×10^2	2.721×10^2	1.325×10^2	2.483×10^1
30	4.693×10^2	3.946×10^2	9.776×10^1	4.720×10^1
40	5.256×10^2	5.054×10^2	1.420×10^2	5.887×10^1
50	5.711×10^2	5.881×10^2	1.709×10^2	7.612×10^1
60–90	5.634×10^2	6.218×10^2	1.773×10^2	7.891×10^1

* Nuclear disintegration rates in the atmosphere, s (g^{-1} yr^{-1}), estimated by Lal and Peters [2] are fitted to a third-order polynomial in altitude, y (km); $s = a1 + a2 \cdot y + a3 \cdot y^2 + a4 \cdot y^3$ for different geomagnetic latitudes.

TABLE 3

Approximate production rates of ^{3}He, neon and argon isotopes from selected targets at sea-level, $\lambda \geqslant 60°$

Target	Nuclide production rate (atoms/g yr)					
	^{3}He *	^{20}Ne	^{21}Ne	^{22}Ne	^{36}Ar	^{38}Ar
O	8.3×10^{1}	–	–	–	–	–
Mg	5.0×10^{1}	8.0×10^{1}	1.1×10^{2}	–	–	–
Al	4.7×10^{1}	2.8×10^{1}	2.4×10^{1}	–	–	–
Si	6.6×10^{1}	3.3×10^{1}	1.8×10^{1}	2.0×10^{1}	–	–
Ca	–	–	–	–	6.9×10^{1}	2.0×10^{2}
Fe	2.8×10^{1}	2.2×10^{-1}	2.4×10^{-1}	2.3×10^{-1}	1.2	1.7

* Includes contribution from decay of ^{3}H.

studies of Cerling (7) yielded a consistent value of 107 ± 3 ^{3}He atoms/(g yr) for sea level and high latitudes, for Tabernacle Hill (Utah) and Bonneville flood (Idaho) rocks of ^{14}C exposure ages 14.4 kyr and 14.5 kyr respectively. Cerling [priv. commun.] has now revised this value based on their true exposure age of ca. 18.0 kyr, obtained using the U-Th coral-calibration of ^{14}C chronology. The revised value for ^{3}He production rate is 107 ± 4 atoms/(g yr). Cerling (priv. commun.) also obtained an internally consistent mean value of 87 ± 6 ^{3}He atoms/(g yr) at sea level and high latitudes for five rocks of 2300–12,200 yr exposure age. This agrees with the value of 82 ± 22 ^{3}He atoms/(g yr) obtained by Kurz et al. [6] for rocks of 2000–7000 yr exposure age, but is about half of the two other estimates of Kurz et al. [6]. It remains to be ascertained whether the large temporal variation observed by Kurz et al. is real.

In view of the current interest in the study of the stable *in situ* produced nuclides, we have theoretically estimated the production rates of ^{3}He, neon and argon isotopes from selected targets. *These estimates must be considered tentative since they are largely based on proton excitation functions; here also the data are limited.* Nevertheless, they are useful since they can also be used to deduce the relative variation in the production rate with target composition. The results are given in Table 3. The cross-section data used are those compiled by Lavielle et al. [25]. In the case of ^{3}He, we have also used the earlier cross-section data for O and N based on direct observations of emissions of protons, deutrons and tritons in cloud chambers [2,23]. It must be noted that the proton excitation functions are quite satisfactory for high threshold reactions, e.g. production of Ne isotopes from Si, Ca and Fe, and Ar isotopes from Fe.

The estimated production rates of ^{3}He (total, including ^{3}H), Ne and Ar isotopes are given in Table 3.

The production rates in Table 3 are for geomagnetic latitudes $\geqslant 60°$ and atmospheric depth, 685 g cm^{-2} (3.34 km). They can be scaled to any altitude, latitude by using the nuclear disintegration polynomials given in Table 2.

The calculations above should be treated as approximate, with possible uncertainties of $\geqslant$ (25–30)%. However, as mentioned earlier, they can be used to give a fair idea of the relative changes in nuclide production rates in different composition minerals, e.g. olivines and pyroxenes of different iron content. The calculated ^{3}He (total) production rates in Mg_2SiO_4, Fe_2SiO_4, $MgSiO_3$ and $FeSiO_3$ at sea level and high latitudes are 68.4, 50.8, 70.0 and 56.4 atoms/(g yr), respectively based on Table 3. The estimates for Mg_2SiO_4 are lower than those obtained experimentally from measurements of ^{3}He in olivines of "known" exposure histories [6,7]; they lie in the bracket (80–190) ^{3}He atoms/(g yr), at sea level and high latitudes, as mentioned earlier. Even compared to the lower estimate, the theoretical value is smaller by $\sim 20\%$. The discrepancy between theoretical and experimental estimates, and the divergence in the experimental data possibly indicates that there may be some other source(s) of ^{3}He production not considered in the calculations, e.g. from low-energy cosmogenic and radiogenic nuclear reactions in light elements, e.g. lithium [20]. Only a

part of the discrepancy could be attributed to uncertainties in cross-section values.

2.4. *Dependence of nuclide production rate on geomagnetic dipole field*

Changes in the dipole field result in a redistribution of the cut-off energies at different latitudes. The global production rates of ^{14}C and ^{10}Be in the atmosphere have been calculated for different dipole field intensities [26,27]. The nuclear disintegration depth profiles in the atmosphere for any given dipole field can similarly be derived from the depth profiles for the present dipole field; see also Nishiizumi et al. [4] who estimated *in situ* nuclide production rates in the Sierra Nevada rocks for hypothetical changes in dipole field. In Fig. 1, I present the estimated changes in the nuclear disintegration rates in the atmosphere at 3.5 km altitude as a function of geomagnetic latitude. Changes in the nuclide production rates are seen to be latitude dependant as expected; maximum change occurs at equator, about +68% for a 50% decrease in the dipole field intensity and −28% for doubling of the field intensity. Consequently, for determining changes in the dipole field strength based on *in situ* nuclides in rocks, samples irradiated at low latitudes should be studied. Reference is made to Kurz et al. [6] who examined *in situ* ^{3}He data in Hawaiian lavas in terms of a temporal change in the earth's dipole field.

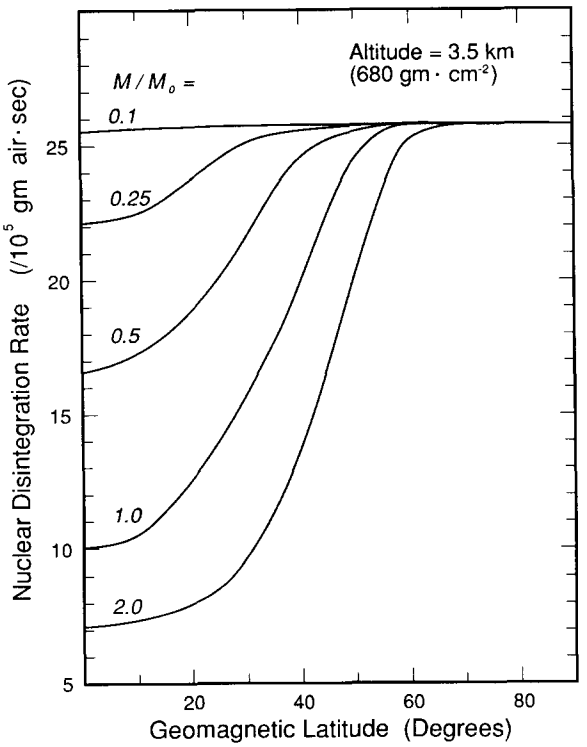

Fig. 1. Total nuclear disintegration rate at 3.5 km (680 g cm^{-2}), due to nucleons of $E > 40$ MeV is given as a function of geomagnetic latitude for different intensities of the earth's dipole field, M; the present field is designated by M_0. The data are from Lal and Peters [2].

2.5. *Depth variation in nuclear reaction rates within a rock*

Experimental data are available for the absorption mean free paths of cosmic ray particles in different absorbers exposed at sea level and at mountain altitudes [28,29]. The values fall in the range 150–200 g cm^{-2} for carbon, air and aluminum and 300–350 g cm^{-2} for lead. The individual measurements have however large uncertainties. The most accurately known are the nuclear absorption mean free paths for the atmosphere, based on measurements of fluxes of slow neutrons. The measured values for the 0–10 km altitudes increase progressively from 150 g cm^{-2} at geomagnetic latitudes 60–90° to 220 g cm^{-2} at equator [2]. This is expected also since the energy spectrum of the high energy parent nucleons ($E >$ 400 MeV), is harder at lower latitudes. The absorption mean free paths for nuclear disintegrations produced in the atmosphere by nucleons of energy, $E > 40$ MeV [2], are given below in Table 4 for 0, 30 and $\geqslant 60°$ geomagnetic latitudes for 0–5 and 5–10 km altitudes. These values are smaller than those for absorption of slow neutrons in the atmosphere, by up to 30% at 0, and are more narrowly confined, 140–175 g cm^{-2}.

TABLE 4

Absorption mean free paths for nuclear disintegrations in the atmosphere ($E > 40$ MeV)

Altitude interval	Mean free path (g cm^{-2})		
	0°	30°	$\geqslant 60°$
0–5 km	160	150	140
5–10 km	175	160	150

The total rate of nuclear interactions in any target can be obtained by scaling the atmospheric production rate at that point by the $A^{2/3}$ factor, where A is the atomic mass number of the target. Within the target, the rate will decrease essentially with an absorption mean free path observed in the atmosphere at that altitude and latitude. In denser targets, e.g. common rock types, the absorption mean free path may be somewhat higher since charged pions (which decay in the atmosphere) produce nuclear disintegrations in condensed materials [2]. The different is expected to be $<$ 20%. This is validated by the fact the mean absorption length for production of ^{10}Be, ^{36}Cl and ^{26}Al in lunar samples at 150–400 g cm^{-2} depth (where the energy spectrum is much harder relative to that in the troposphere at $\lambda \geq 60°$) is ~ 175 ($\pm 5\%$) g cm^{-2} [30]. This value is close (within 15%) to the value of 150 g cm^{-2} observed in the upper troposphere at latitudes $\geq 60°$. This comparison leads us to the conclusion that the absorption mean free path in typical rocks may at most be up to 10% higher than in the atmosphere; i.e. lie in the range of 175–155 g cm^{-2} for 0–5 km altitudes for the 0–90° latitude interval.

3. Interpretation of in situ cosmogenic radionuclide data

The central basis of study of surficial processes with the *in situ* radionuclides is the appreciable attenuation of cosmic ray energy and flux in traversing through matter due to nuclear interactions and ionization losses. At depths in the atmosphere exceeding 200 g cm^{-2} (0–10 km altitude) the nuclear cascade primarily shows an exponential attenuation, with little change in the energy spectrum of nuclear active particles, primarily neutrons and protons [28,1]. The absorption mean free path is however latitude dependent. Consequently, the rate of nuclear disintegrations, and therefore also the radionuclide production rate decreases exponentially with depth inside a target. For a flat geometry target exposed with its surface horizontally, the production rate of a radionuclide, P (atoms/g s) varies with depth, x (cm):

$$P(x) = P(0)\, e^{-\rho x/\Lambda} \tag{2}$$

$$P(x) = P(0)\, e^{-\mu x} \tag{2'}$$

where ρ is the mean density of the target rock (g cm^{-3}) and Λ is the absorption mean free path for nuclear interacting particles in the target (g cm^{-2}) of density ρ (g cm^{-3}). $P(0)$ is the production rate of the radionuclide at the target surface. In equation (2′), the symbol μ is defined as the absorption coefficient (cm^{-1}) in the target; $\mu = \rho/\Lambda$. The accumulation of radionuclide in a rock horizon can now be easily calculated for a flat geometry rock (for complex target geometries, the cosmic ray attenuation has to be calculated on a case by case basis as was done in the case of Sierra Nevada rocks [4]. The number of atoms of the radionuclide within the rock at any depth, x, $N(x,t)$ is given by the differential equation:

$$\frac{dN(x,t)}{dt} = -N(x,t)\lambda + P(x,t) \tag{3}$$

with

$$P(x,t) = P(0,t)\, e^{-\mu x(t)} \tag{4}$$

In the above, implicit is the assumption that the radionuclide (λ = disintegration constant) is produced only by cosmic ray nucleons and that the production is fairly well characterized by an exponential depth decrease with an absorption mean free path, $1/\mu$ (cm). If the nuclide is produced by muons and radiogenic reactions the absorption mean free path would be depth dependent. Equation (4) is an alternate form of eqn. (2). The erosion rate $\epsilon(t)$, defines the value of $x(t)$ according to the equation:

$$x(t) \int_0^t \epsilon(t)\, dt + \text{const.} \tag{5}$$

We will first consider the simple case of $\epsilon(t)$ = constant = ϵ; *also for our present purposes, it would suffice to treat the cosmic ray intensity as a constant*, i.e. $P(x,t) = P(x)$. For equation (3) one then obtains the following solution for the concentration $N(x,t)$ in a sample at depth, x:

$$N(x,t) = N(x,0)\, e^{-\lambda t} + \frac{P(0)}{\lambda + \mu\epsilon}\, e^{-\mu x}(1 - e^{-(\lambda+\mu\epsilon)t}) \tag{6}$$

where $N(x,0)$ is the initial number of atoms/g in the rock surface now at depth, x, after an irradiation for a time period, t.

3.1. Steady-state erosion

For a continuous *long-term irradiation*, i.e. $t \gg 1/(\lambda + \mu\epsilon)$, equation (6) reduces to either of the two equations:

$$N(x,t) = N(x,0)\, e^{-\lambda t} + e^{-\mu x}\frac{P(0)}{\lambda + \mu\epsilon} \tag{7}$$

$$N(x,t) = e^{-\mu x}\frac{P(0)}{\lambda + \mu\epsilon} \tag{8}$$

Equation (8) corresponds to the special case of a rock horizon eroding in *steady state*, since the concentration of the radionuclide in the present rock surface was initially zero when it was deep seated and shielded from cosmic radiation. Equation (7) holds when the present rock surface was not shielded sufficiently from cosmic radiation at $t = 0$, and should be considered as an exception rather than the rule.

Equation (8) states that if a rock surface undergoes a *steady state erosion*, the *in situ* radionuclides attain the secular equilibrium concentration corresponding to an effective disintegration constant, $\lambda + \mu\epsilon$. The effective irradiation time, T_{eff} for the top surface of the rock ($x = 0$) is then given by:

$$T_{\text{eff}} = \frac{1}{\lambda + \mu\epsilon} \tag{9}$$

$$T_{\text{eff}} = \frac{N(0)}{P(0)} \tag{10}$$

where $N(0)$ denotes the nuclide concentration in the top surface of the rock for the case of a steady-state erosion and cosmic ray irradiation after a long time $t \gg 1/(\lambda + \mu\epsilon)$.

The validity of the steady-state model for a rock surface can be tested by studying two radionuclides of different half-lives; the sensitivity of this test would depend on the magnitude of difference between the terms $\lambda_1 + \mu\epsilon$ and $\lambda_2 + \mu\epsilon$ for radionuclides of disintegration constants, λ_1 and λ_2. The model steady-state erosion rate, ϵ, is given by:

$$\epsilon = \frac{1}{\mu}\left[\frac{P}{N} - \lambda\right] \tag{11}$$

where the quantity is $(P/N - \lambda)$ *invariant* for different isotopes:

$$\left(\frac{P}{N}\right)_1 - \lambda_1 = \left(\frac{P}{N}\right)_2 - \lambda_2 = \left(\frac{P}{N}\right)_3 - \lambda_3 \tag{12}$$

In equations (11) and (12), we have used the symbols P and N for $P(0)$ and $N(0)$, for simplicity.

If equation (12) holds for different isotopes, the erosional surface can be stated to have been in a steady state over time periods of up to (3–5) $\times T_{\text{eff}}$, where T_{eff} is given by eqn. (9). Note however that if $1/\mu$ is very large compared to ϵ, in which case $T_{\text{eff}} \approx P/N \approx 1/\lambda$, and no information can be had about ϵ. Validity of eqn. (12) would not necessarily imply that the surface has been undergoing continuous erosion on a micro-scale. The rock surface may have undergone sporadic mass-wastage due to fragmentation and chip-off of layers of varying thicknesses during time periods of the order of T_{eff}. But the validity of the invariant relation would assert that the last chip-off distance was considerably smaller than the mean cosmic ray absorption length ($1/\mu$), of the order of 50 cm.

3.1.1. Concepts of apparent erosion rates and apparent surface exposure ages

In an erosional surface, the top surface of a rock is continually being replaced by a layer just below the surface. In a continuously eroding surface, it would be useful to obtain some estimates of (1) the mean erosion rate, $\bar{\epsilon}$, over specified time intervals in the past and the complimentary parameter, and (2) the surface exposure age, T_{eff}. Whereas it would seem justifiable to obtain some operational value of $\bar{\epsilon}$, one may not at first glance see any justification for defining T_{eff} since the top surface is continually being replaced by deeper seated layers. However, as discussed below, this is a justifiable parameter and it has a well defined meaning. We will first discuss the significance of T_{eff} for the case of steady state, i.e. constant erosion rate over a period of time, $t \gg (\lambda + \mu\epsilon)$; see equation (6). In this case $\bar{\epsilon} = \epsilon$ and $N(0) = P(0)/(\lambda + \mu\epsilon)$; equation (8). This is analogous to the secular equilibrium build up with production for a nuclide of mean life, $1/(\lambda + \mu\epsilon)$, the effective number of years over which the concentration of this nuclide would build up in a

sample exposed at the surface, in the absence of decay and erosion. In other words, the effective surface exposure age of the rock, T_{eff}, is given by:

$$T_{\text{eff}} = \frac{N(0)}{P(0)} = \frac{1}{(\lambda + \mu\epsilon)} \tag{13}$$

and erosion rate is related to T_{eff} by:

$$\epsilon = \frac{1}{\mu}\left[\frac{1}{T_{\text{eff}}} - \lambda\right] \tag{14}$$

Clearly the surface exposure age thus obtained (eqn. 13) must be defined either as the *effective*, preferably *apparent* surface exposure age. An estimate of T_{eff} based on one nuclide has implicit in it the assumption of a steady state. If data are available for more than one nuclide of widely different half-lives, one may be able to check on the validity of the steady-state erosion model. As noted above the *effective mean life* of a nuclide depends on the rate of erosion. The time intervals over which the validity of the steady-state erosion model can be checked is defined by the individual effective mean lives of the nuclides, $1/(\lambda_1 + \mu\epsilon)$, $1/(\lambda_2 + \mu\epsilon)$, etc. Clearly, if the value of $\mu\epsilon$ is much smaller or greater than both λ_1 and λ_2, one cannot check on the validity of the steady-state erosion model.

The suitability of a given radionuclide to determine the rate of erosion of a given horizon is thus determined by the condition that λ and me should be of the same order; in other words T_{eff} and the mean life of the radionuclide should be of the same order. If $\lambda \gg \mu\epsilon$, the radionuclide would be built to its secular equilibrium value ($T_{\text{eff}} = 1/\lambda$) and no information can be obtained from its study about the erosion rate. Else if $\mu\epsilon \gg 1$, the nuclide concentrations build up to the same concentration independent of the half-life of the radionuclide. The rock dynamics then determines the nuclide build-up; i.e. the nuclide decay during the build-up period is unimportant and the nuclide behaves as a stable one. In this case the apparent surface exposure age, $T_{\text{eff}} = 1/\mu\epsilon$, i.e. it is the time during which erosion removes a rock depth equivalent to one absorption mean free path for cosmic rays, $1/\mu$, ~ 50 cm in common rocks. And the erosion rate, ϵ and the effective exposure, T_{eff} age are related by the expression:

$$\epsilon = \frac{1}{\mu T_{\text{eff}}} \tag{15}$$

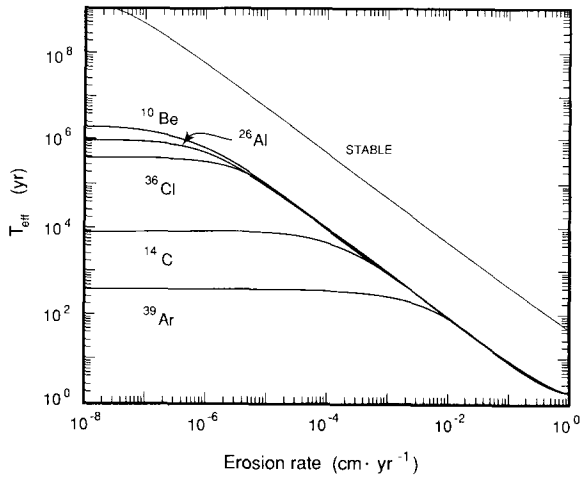

Fig. 2. Calculated values of effective surface exposure ages, T_{eff} as a function of erosion rate for five radionuclides and a stable nuclide.

$$\sim \frac{50}{T_{\text{eff}}} \tag{16}$$

The ϵ, λ, T_{eff} relationships for a steady-state erosion (eqn. 9) are shown graphically in Fig. 2 for a stable nuclide and the five radionuclides which can be conveniently employed for erosion studies.

3.2. *Non-steady state erosion*

In the absence of *in situ* data on several radionuclides, the only meaningful model calculation one has to resort to is the steady-state erosion model (eqn. 9). And since the erosional process is not generally expected to be a continuous one and occurring at a uniform rate of erosion, it would be useful to consider what the implications are of the calculated model erosion rate. We discuss below that one can place some plausible limit on the erosion rate based on studies of even one *in situ* radionuclide. The situation improves considerably if two *in situ* radionuclides are studied. Our approach is based on probabilistic considerations, and its application assumes that the rock surface studied is not too unrepresentative of the average rock surface in that horizon. Essentially, it implies that the researcher has measured the same radionuclide in several surfaces from the region to confirm the representative character of the surfaces studied. We discuss below the implications of the *in situ* data separately for one and two or more radionuclides.

3.2.1. Data on a single radionuclide

In this case, the assumption of a steady-state uniform erosion of the surface leads to a model erosion rate based on eqn. (11). We may distinguish two cases here: the effective exposure age of the rock is (a) small compared to the radionuclide mean life or (b) comparable to the mean life; see Fig. 2. In the latter case, one can assert that the maximum value of the time averaged erosion rate (on time scale $\sim T_{\text{eff}}$), $\bar{\epsilon}$, is of the order of $\leqslant \lambda/\mu$. In the context of geomorphology, this would be very valuable information if radionuclides of half-lives exceeding few hundred years are used.

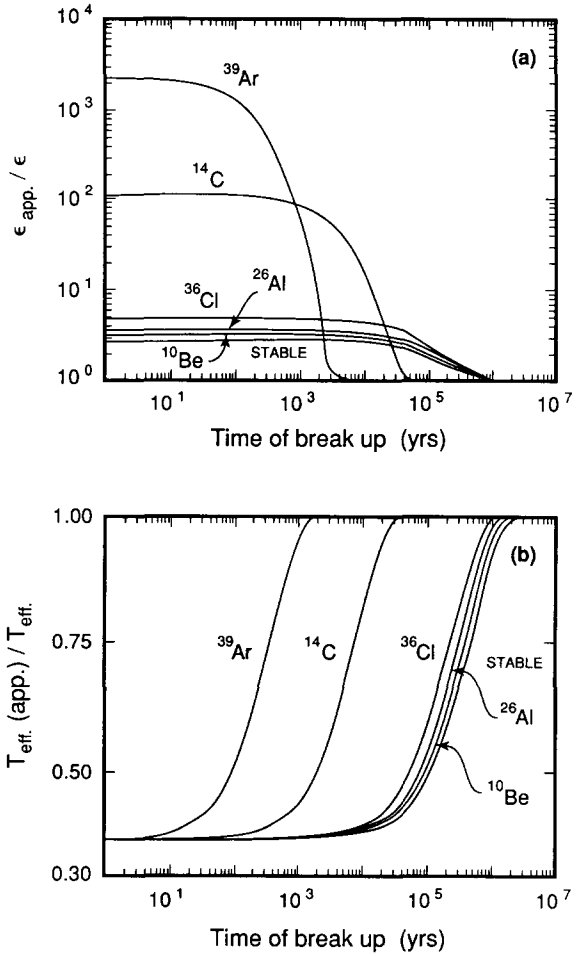

Fig. 3. Calculated values of the ratios of "apparent" and "true" erosion rates are plotted in (a) as a function of the time of break-up of a top layer of thickness, 50 cm; the erosion rate was assumed to be 10^{-4} cm yr^{-1} before and after the break-up. In (b), the ratios of "apparent" and "true" effective surface exposure ages are given for the same irradiation history as in (a).

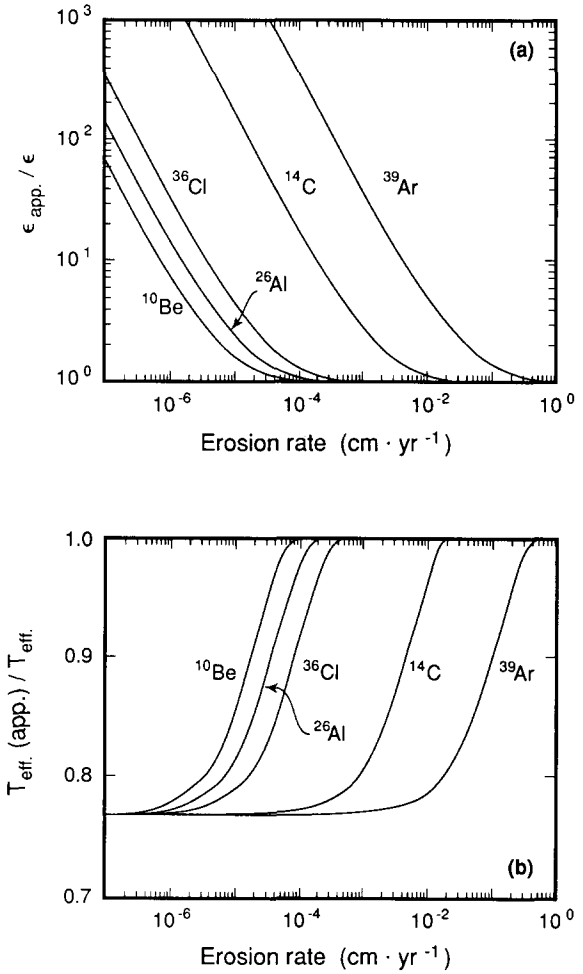

Fig. 4. The calculated ratios of "apparent" and "true" erosion rates are given in (a) as a function of erosion rate for five different radionuclides, for a break up of a top layer of 50 cm one mean life ago. In (b), the ratios of "apparent" and "true" effective surface exposure ages are plotted against erosion rate for the same irradiation history as in (a).

If, however, the effective exposure period, T_{eff} is $\sim 1/\lambda$ then the model erosion rate should of course be considered to be an upper limit on the average erosion rate. The same is true even if $T_{\text{eff}} < 1/\lambda$. This follows if one considers the realistic situation of sporadic losses of material from the surface, due to landslide, chip-off, etc. To quantify this discussion, we hypothesize that the surface underwent a loss of Δx cm, T yr. before present and that the rock eroded steadily otherwise at a uniform rate. In Fig. 3a we have plotted the ratio

$\epsilon_{app}/\epsilon_{true}$ for five radionuclides, ^{39}Ar, ^{14}C, ^{36}Cl, ^{26}Al and ^{10}Be, as a function of time of chip-off, T. For our calculations, we assumed $\Delta x = 50$ cm, i.e. close to the cosmic ray absorption mean free path in rock, and $\epsilon_{true} = 10^{-4}$ cm yr^{-1}. It is seen that the longer lived the radionuclide, the lesser one overestimates the erosion rate. Thus, the use of a single radionuclide can lead to a considerable overestimation of the erosion rate for shorter half-life radionuclides. The corresponding ratios of T_{eff} (apparent)/T_{eff} (true) for different break up times are plotted in Fig. 3b; the limiting value of the ratio is determined by the value of Δx.

I propose that for a single radionuclide, a good bracket of the erosion rate would be that between the steady state equation and an assumption of a chip-off of 50 cm of rock from the surface, one mean life ago. This also seems to be a quite plausible guess for the hypothetical chip-off parameters. In Fig. 4 we have plotted the corresponding calculated values of $\epsilon_{app}/\epsilon_{true}$ and T_{eff} (apparent)/T_{eff} (true) as a function of ϵ_{true}. It is seen that provided $\lambda \sim \mu\epsilon$, the erosion rate is estimated fairly accurately, but large errors (overestimates) can occur if $\lambda \gg \mu\epsilon$, as we already noted earlier; see Fig. 3.

3.2.2. *Data for two in situ* radionuclides

The ratio of concentrations of two radionuclides in an eroding horizon changes sensitively with the rate of erosion [8]. At steady state, the ratio of concentrations of two radionuclides, i and j at the rock surface is given by the equation:

$$R_{ij}(0) = N_i(0)/N_j(0) = \frac{P_i(0)}{P_j(0)} \frac{\lambda_j + \mu\epsilon}{\lambda_i + \mu\epsilon} \tag{17}$$

$$= \frac{P_i(0)}{N_j(0)} \frac{1}{\left(P_j(0)/N_j(0)\right) + \lambda_i - \lambda_j} \tag{17'}$$

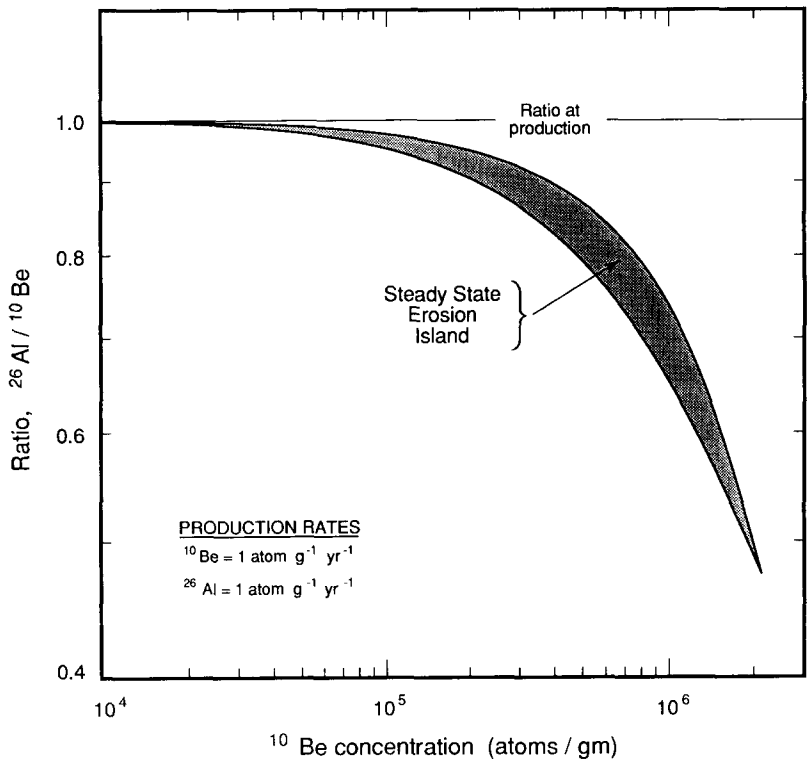

Fig. 5. The theoretically calculated build up of the ratios of ^{10}Be and ^{26}Al are plotted as a function of ^{10}Be concentration for a steady-state irradiation history, with and without erosion, for unit nuclide production rates. The upper bound of the curve is traced by irradiating a rock of zero erosion. Rocks of different erosion rates populate the stippled zone, termed the *steady-state erosion island*, for the case of constant erosion rates.

A plot of $N_i(0)$ vs. $R_{ij}(0)$ is a smoothly varying function reaching an end point at:

$$N_i(0) = P(0)/\lambda_i, \quad \text{and } R_{ij}(0) = \frac{P_i(0)\cdot\lambda_j}{P_j(0)\cdot\lambda_i} \quad (18)$$

corresponding to the case of $\epsilon = 0$. In Fig. 5 we have plotted the expected behavior for the pair ^{26}Al and ^{10}Be. Since we are considering the ratio of a shorter half-life nuclide to a longer half-life nuclide, the ratio steadily decreases as ϵ decreases (see Fig. 2). The families of curves have an upper envelope obtained for the case of irradiation of a zero erosion rock horizon (*with zero initial concentration*), for different time periods. In this case, the concentration of a radionuclide varies with time according to the relation:

$${}_0N_i(0,t) = \frac{P_i}{\lambda_i}(1 - e^{-\lambda_i t}) \quad (19)$$

The ratio ${}_0N_i(0,t)/{}_0N_j(0,t)$ after t years of irradiation is then given by:

$${}_0R_{ij}(0,t) = \frac{1}{{}_0N_j(0,t)}\frac{P_i}{\lambda_i}\left[1 - \left(1 - {}_0N_j(0,t)\frac{\lambda_j}{P_j}\right)^{\lambda_i/\lambda_j}\right] \quad (20)$$

where the subscript on the left hand side denotes that $\epsilon = 0$. Any eroding rock surface will have radionuclide concentrations given by the zone bounded on the top by the no-erosion case considered above (eqn. 20) and the lower line (eqn. 17′); this is shown in Fig. 5, starting from the ordinate at P_i/P_j and ending at the ordinate, $[P_i(0)/P_j(0)](\lambda_j/\lambda_i)$, according to equation (18). The zone bounded by these cases is shown in Fig. 5 for $P_i(0) = P_j(0) = 1$ atom/(g yr). I call this zone the *steady-state erosion island* since all steady-state erosional histories will plot within this island.

In Fig. 6, I have shown the steady-state zero erosion line build-up curve for ^{26}Al and ^{10}Be, again for unit production rates. If the rock surface, after it has attained certain ^{26}Al, ^{10}xe concentrations is shielded from cosmic radiation (e.g. due to burial), the ratio–concentration profile would evolve along the straight lines drawn at about 75° in Fig. 6. [It can be shown that if the concentration of two radionuclides i and j are $C_i(0)$ and $C_j(0)$ at $t = 0$, then the ratio $C_i(t)/C_j(t)$ varies as $[C_j(t)]^{(\lambda_i-\lambda_j)/\lambda_i}$ due to decay with time in the case of no production. This explains why the ratio vs. concentration is a straight line on a log-log plot (Fig. 6).] Iso-time lines are also drawn in Fig. 6. In this figure, the stippled zone denotes the forbidden zone; any datum lying in this zone would indicate either a measurement error (or a contamination of the sample). This holds as long as the cosmic ray intensity at the site does not increase. However if the sample received prior exposure at a site where the nuclide production rate was higher, the datum can lie in the forbidden zone. Any burial of the sample would only result in an effective decrease in cosmic ray intensity. Lowering of the cosmic ray intensity can arise due to change in the primary cosmic ray flux and/or due to elevation change due to tectonic activity. Alternately the sample could have been irradiated at a higher altitude and later on transported to a lower altitude.

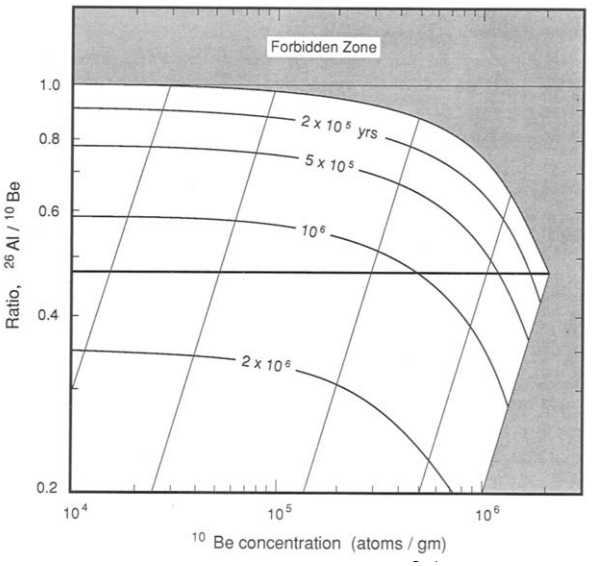

Fig. 6. The upper bound of the curve is for the case of irradiation of a zero erosion rock surface as in Fig. 5. The straight lines denote the path traced by the rock samples for ^{10}Be and ^{26}Al concentrations for rocks are shielded from cosmic radiation after reaching the different points on the upper curve. Production rates of ^{10}Be and ^{26}Al are fixed at 1 atom/g yr.

Locations in the allowed zone of Fig. 6 can be reached in a variety of ways. In Fig. 7 we have considered two cases of nuclide concentration evolution. Initially the rock surfaces are allowed to reach ^{10}Be concentrations of 10^5, 5×10^5, $1.5 \times$

10^6 and 2.1×10^6 atoms/g (for unit production rates of two nuclides). Subsequently the rock surface is shielded by a sedimentary cover which remains fixed in time; i.e. the production of nuclide continues in the rock surface at a constant rate. In Fig. 7, we have considered shielding to reduce production rates at the test surface by a factor of four (case labeled 1 in Fig. 7) and ten (case labelled 2). As seen from Fig. 7, the curves evolve finally reaching a point on the horizontal line at final ^{10}Be concentrations of $1/4\times$ and $1/10\times$ the final concentrations of ^{10}Be for the case of unit production, as would be expected also.

The above examples serve to illustrate how the nuclide concentration versus ratio curves evolve for two nuclides in the case of different non-steady state erosion situations, compared to the case of steady-state erosion, for which the evolution of the curve is confined within the erosion island. Clearly the evolution can proceed in a number of different ways, but the trajectories considered do give a fair idea of how they evolve with time for different irradiation histories. Samples lying within the allowed zone can reach that state in a variety of ways, e.g. by a complex irradiation of erosion and burial. However, based on geophysical considerations, one can possibly rule out certain irradiation trajectories, e.g. those which involve a very long irradiation history. The irradiation history scenarios can thus be appreciably constrained if data are available for two or more *in situ* radionuclides of suitable half-lives. (The approach followed here is similar to that adopted earlier for the study of irradiation histories of air masses [2]. Reference is also made to a similar analysis by Klein et al. [31] of the *in situ* ^{10}Be and ^{26}Al data in Libyan glass.)

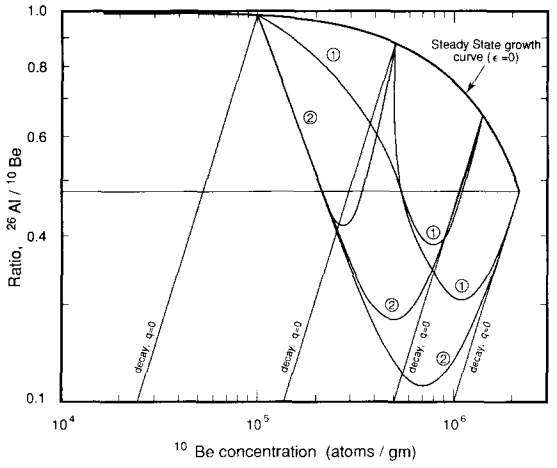

Fig. 7. More complex irradiation histories than in Fig. 7 showing evolution of ^{26}Al/^{10}Be ratios with ^{10}Be concentration; the decay lines ($q = 0$), as in Fig. 6 are also shown. Curves marked (*1*) and (*2*) correspond to continued cosmic ray irradiation of the surface after attaining ^{10}Be concentrations of 10^5, 5×10^5, 1.5×10^6 and 2.1×10^6 atoms/g with cosmic ray flux reduced by factors of 4 and 10 respectively due to sedimentation on the surface. For simplicity, production rates of ^{10}Be and ^{26}Al are fixed at 1 atom/g yr, as in Figs. 5 and 6.

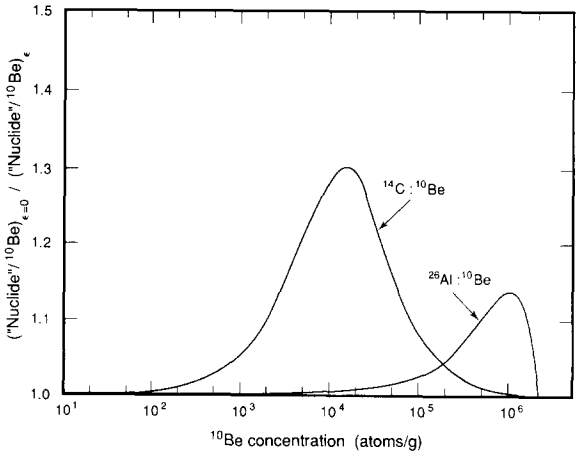

Fig. 8. The ratio of ratios of the concentration of a nuclide and ^{10}Be, without and with erosion (for different erosion rates) is plotted as a function of ^{10}Be concentration for the case of irradiation of a rock horizon with zero initial concentrations of these nuclides. All calculations refer to the nuclide concentrations measured in the exposed rock surface, and unit production rates of the nuclides.

The ratio of concentrations of two radionuclides attained for the case of $\epsilon = 0$ relative to the ratio for finite ϵ, when plotted as a function of the concentration of one of the radionuclides shows a transition. As an illustration, in Fig. 8 we have plotted $(\text{nuclide}/^{10}\text{Be})_{\epsilon=0}/(\text{nuclide}/^{10}\text{Be})_{\epsilon}$ ratios as a function of ^{10}Be concentrations, for ^{14}C and ^{26}Al. The maximum values attained by the ratio of ratios are 1.3 and 1.14 respectively.

4. Modeling elevation changes during irradiation

So far we have tacitly assumed that the cosmic ray flux remained constant during the rock's irradiation history. It would be of interest to see the magnitude of changes expected in nuclide concentrations if the exposed rock underwent changes in elevation due to tectonic activity. The

polynomial expression used for nuclide production rate as a function of altitude (eqn. 1) does not lead to a simple analytical function on solving eqn. (3) to explicitly show the effect of elevation changes vis-a-vis the effect of rock erosion. However, one can estimate the effect by making the approximation that over a limited range of altitude, the production rate varies exponentially with altitude. In that case the effects of erosion and elevation changes are similar (cf. eqns. 4 and 8) and one obtains a simple expression for the steady-state concentration of a radionuclide in the presence of constant erosion and uplift or subduction:

$$N(0) = \frac{P(0)}{\lambda + \mu\epsilon + \beta/H} \tag{21}$$

where β is the rate of change of elevation and H is the mean scale height for the production of the nuclide. Reference is made to Craig and Poreda [9] for discussion of elevation change in context to He^3 produced in rocks. The inverse of the mean scale height, H at any latitude in the troposphere is given by $(1/q)(dq/dy)$ and is easily obtained from the polynomial coefficients in Tables 1 or 2. In Fig. 9 we have plotted the calculated scale heights for total nuclear disintegration rates in the 0–5 km interval, for 0, 30 and $\geqslant 60°$ geomagnetic latitudes. It is seen that the scale height H varies appreciably with altitude, invalidating the oversimplification made in deriving eqn. 21, but for the purposes of seeing the effect of elevation changes, it is quite adequate.

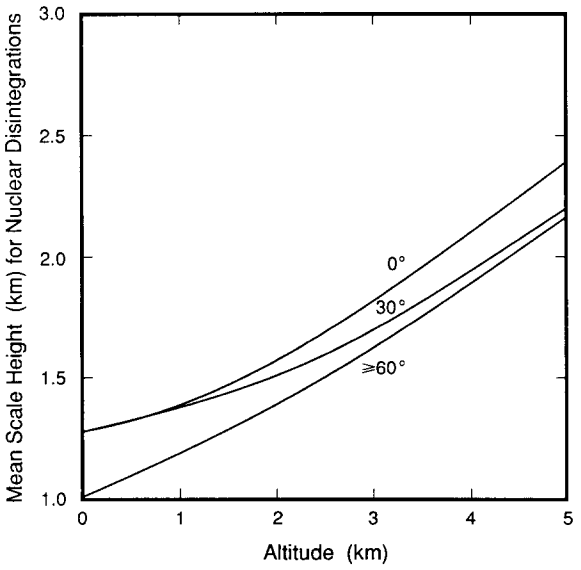

Fig. 9. The mean scale height (km) for nuclear disintegrations as a function of altitude for 0, 30 and $\geqslant 60$ geomagnetic latitudes, for 0–5 km altitudes.

The effect of elevation change is to add a term β/H in the denominator whereby if β is positive, one overestimates the erosion rate if the effect of elevation change is ignored, and vice versa. For the effect of the elevation to be as important as that of erosion, $\mu\epsilon \sim \beta/H$, or $\beta \sim \mu H\epsilon$. From Fig. 9, we see that H is of the order of 1–2 km. Taking a mean value of 1.5 km, the rate of elevation change, β should be about 3×10^3 ϵ to be as important as erosion in determining the steady-state nuclide concentration.

This exercise shows that one cannot determine the elevation change rate from *in situ* nuclides except when the rock erosion rates are very low. In real situations, in regions of high uplift rate, say 0.1–1 cm yr^{-1} one also observes erosion rates exceeding 0.1 cm yr^{-1} whereby the erosion term in the denominator of eqn. (21) is at least 10^3 times greater than the elevation term. If the value of e exceeds 0.01 β, which seems to be valid in most cases, the *in situ* nuclide build up would be primarily determined by erosion.

5. Errors in estimation of ϵ and T_{eff}

It would be useful to discuss briefly the statistical errors in estimating the erosional parameters due to uncertainties in the nuclide production rates and concentrations, assuming the validity of the erosion model. In the case of a single nuclide, the fractional error in ϵ, relative to fractional error in estimation of $P(0)$ or $N(0)$ is given by:

$$\left(\frac{\partial\epsilon}{\epsilon}\right)\Big/\left(\frac{\partial P(0)}{P(0)}\right) = \left(\frac{\partial\epsilon}{\epsilon}\right)\Big/\left(\frac{\partial N(0)}{N(0)}\right)$$

$$= \frac{1}{1 - \lambda N(0)/P(0)} \tag{22}$$

$$= \frac{1}{1 - \lambda T_{\text{eff}}} \tag{23}$$

Relation (22) shows that the fractional error in ϵ increases with fractional error in $N(0)$ or $P(0)$. Furthermore, when λ $N(0) \sim P(0)$ the errors in e become very large. An alternate way of expressing

this is that when the apparent surface exposure age, $T_{\text{eff}} \sim 1/\lambda$, the errors in ϵ are very large (eqn. 23), and consequently one has to chose a different nuclide (of longer half-life) for studying the erosion rate. The fractional errors in determining T_{eff} are given by the following expressions:

$$\frac{\partial T_{\text{eff}}}{T_{\text{eff}}} = \frac{\partial N(0)}{N(0)} \tag{24}$$

$$\frac{\partial T_{\text{eff}}}{T_{\text{eff}}} = -\frac{\partial P(0)}{P(0)} \tag{25}$$

If ratio of two radionuclides is used to determine the erosion rate (eqn. 17), then the situation is opposite of that for the case of concentration of a single radionuclide. Rewriting eqn. (17),

$$\epsilon = \frac{\lambda_j - k\lambda_i}{\mu(k-1)} \tag{26}$$

where

$$k = R_{ij}(0)/\left[P_i(0)/P_j(0)\right] \tag{27}$$

The form of eqn. (26) shows that when $k \sim 1$ or $k \sim \lambda_j/\lambda_i$, the errors in e become very large; eqn. (26) can be used satisfactorily for determining ϵ when $1 < k < (\lambda_j/\lambda_i)$.

Considerations such as above are very useful in deciding on the nuclide(s) and the method best suitable to estimate erosion rates.

6. Conclusions

For applying cosmogenic *in situ* nuclides to problems in geomorphology, it is essential to know their production rates under different conditions of exposure to cosmic radiation, as a function of latitude altitude and shielding. I discuss that if the production rate of a nuclide can be determined at any location in the atmosphere for any irradiation geometry, the nuclide production rate can be obtained for different irradiation conditions using the extensive cosmic ray neutron data. These data, believed to be accurate within $\pm 10\%$, have been used by Lal and Peters [2] to estimate relative latitude–altitude variation of rates of nuclear disintegrations of produced by nucleons of energy, $E > 40$ MeV in the atmosphere. Estimates of changes in the nuclide production rates with variations in the geomagnetic dipole field or in the solar activity can easily be made using the procedures discussed.

The production rates of ^{10}Be, ^{26}Al and ^{14}C in quartz have been determined experimentally [4–5] by studying rocks of well constrained irradiation histories. I present estimates of their production rates in quartz exposed at 0–90° latitudes and 0–10 km altitudes in the atmosphere, in terms of a third-degree polynomial by scaling to the nuclear disintegration curves of Lal and Peters [2]. The validity of the ^{10}Be and ^{26}Al production estimates is borne out for the high latitudes (> 60°) and altitudes 1.2–2.6 km by the recent experimental data on a large number of Antarctic rocks many of which exhibit near secular equilibrium irradiation for ^{10}Be and ^{26}Al activities [18].

I have also presented theoretical estimates for the production rates of ^{3}He and isotopes of Ne and Ar from relevant targets; these estimates may be uncertain by > (25–30)% because of lack of cross-section data. The estimated production rates of ^{3}He in olivines are compared with experimental data which yield higher production rates by up to a factor of ~ 2. Disagreement may in part be due to production of ^{3}He by mechanisms other than spallation of Mg, Si and O.

I have discussed a number of cosmic ray irradiation models to characterize the exposure histories of rocks with special reference to five radionuclides, ^{39}Ar, ^{14}C, ^{36}Cl, ^{26}Al and ^{10}Be and stable nuclides. The meaning of apparent erosion rates and apparent surface exposure ages in relation to steady-state irradiation models is discussed. I have also considered the effect of perturbations in the steady state due to sporadic chip-off of a layer from the surface. *In situ* experimental data on ^{10}Be and ^{26}Al validate the usefulness of the models considered [18,31,17]. The results for the Antarctic rocks [18] clearly show the existence of the *erosion island* predicted from the model calculations.

The erosion models emphasise the need to study multiple nuclides to constrain the exposure history of a sample. The five nuclides, ^{14}C, ^{36}Cl, ^{26}Al, ^{10}Be and ^{21}Ne can be conveniently studied in quartz because of its stability and ubiquitous nature.

The radionuclide ^{14}C seems ideally suited for measuring erosion rates in the bracket 10^{-3}–3×10^{-2} cm yr^{-1} (i.e. in the vicinity of $\lambda \sim \mu\epsilon$); such erosion rates are widely encountered. Exceptions are regions of high tectonic activity where $\epsilon > 10^{-1}$ cm yr^{-1} and in Antarctic rocks where very low erosion rates, $10^{-5} \times 10^{-4}$ cm yr^{-1}, have been observed [18].

Acknowledgements

I am thankful to Prof. J. R. Arnold and Drs. J. Klein, C. Kohl, R. Middleton, K. Nishiizumi and R. C. Reedy for useful discussions throughout the development of the *in situ* method for studying irradiation histories of rocks. Thanks are due to Dr. T. Cerling for communicating his unpublished data on ^{3}He production rates. This work was supported by a NSF grant, NSF EAR898-04677.

References

1 D. Lal, *In situ* produced cosmogenic isotopes in terrestrial rocks; Annu. Rev. Earth Planet. Sci. 16, 355–388, 1988.
2 D. Lal and B. Peters, Cosmic ray produced radioactivity on the earth, in: Handbuch der Physik, Vol. XLVI/2, Springer, Berlin, pp. 551–612, 1967.
3 D. Lal, J.R. Arnold and M. Honda, Cosmic ray production rates of ^{7}Be in oxygen and ^{32}P, ^{33}P, ^{35}S in argon at mountain altitudes, Phys. Rev. 118, 1626–1632, 1960.
4 K. Nishiizumi, E.L. Winterer, C.P. Kohl, J. Klein, R. Middleton, D. Lal and J.R. Arnold, Cosmic ray production rates of ^{10}Be and ^{26}Al in quartz from glacially polished rocks, J. Geophys. Res. 94, 17,907–17,915, 1989.
5 A.J.-T. Jull, D.J. Donahue, T.W. Linick and G.C. Wilson, Spallogenic ^{14}C in high-altitude rocks and in Antarctic meteorites, Radiocarbon 32 (in press), 1990.
6 M.D. Kurz, D. Colodner, T.W. Trull, R.B. Moore and K. O'Brien, Cosmic ray exposure dating with in situ produced cosmogenic ^{3}He: results from young Hawaiian lava flows, Earth Planet. Sci. Lett. 97, 177–189, 1990.
7 T.E. Cerling, Dating geomorphologic surfaces using cosmogenic ^{3}He, Quat. Res. 33, 148–156, 1990.
8 D. Lal and J.R. Arnold, Tracing quartz through the environment, Proc. Indian Acad. Sci., Earth Planet. Sci. 94, 1–5, 1985.
9 H. Craig and R.J. Poreda, Cosmogenic ^{3}He in terrestrial rocks: the summit lavas of Maui, Proc. Natl. Acad. Sci. U.S.A. 83, 1970–1974, 1986.
10 M.D. Kurz, Cosmogenic helium in a terrestrial igneous rock, Nature 320, 435–439, 1986.
11 F.M. Phillips, B.D. Leavy, N.O. Jannik, D. Elmore and P.W. Kubik, The accumulation of cosmogenic chlorine-36 in rock: a method for surface exposure dating, Science 231, 41–43, 1986.
12 R. Davis Jr. and O.A. Schaeffer, Chlorine-36 in nature, Ann. N.Y. Acad. Sci. 62, 105–122, 1955.
13 Y. Yokoyama, J. Reyss and F. Guichard, Production of radionuclides by cosmic rays at mountain altitudes, Earth Planet. Sci. Lett. 36, 44–50, 1977.
14 K. Nishiizumi, D. Lal, J. Klein, L. Middleton and J.R. Arnold, Production of ^{10}Be and ^{26}Al by cosmic rays in terrestrial quartz and implications for erosion rates, Nature, 319, 134–136, 1986.
15 F. Yiou, G.M. Raisbeck, J. Klein and R. Middleton, ^{26}Al/^{10}Be in terrestrial impact glasses, J. Non-Cryst. Solids 67, 503–509, 1984.
16 F.M. Phillips, M.G. Zreda, S.S. Smith, D. Elmore, P.W. Kubik and P. Sharma, A cosmogenic chlorine-36 chronology for glacial deposits at Bloody Canyon, Eastern Sierra Nevada, California, Science 248, 1529–1532, 1990.
17 K. Nishiizumi, C.P. Kohl, J. Klein, R. Middleton, D. Lal, J.R. Arnold and R. Dorn, Cosmogenic in situ ^{10}Be, ^{26}Al in rocks from different geographical locations, Unpublished, 1990.
18 K. Nishiizumi, C.P. Kohl, J.R. Arnold, J. Klein, D. Fink and R. Middleton, Cosmic ray produced ^{10}Be and ^{26}Al in Antarctic rocks: exposure and erosion history, Earth Planet. Sci. Lett. 104, 440–454, this issue, 1991.
19 M.G. Zreda, F.M. Phillips, D. Elmore, P.W. Kubik and P. Sharma, Cosmogenic chlorine-36 production rates in terrestrial rocks, Preprint, 1990.
20 D. Lal, Production of ^{3}He in terrestrial rocks, Chem. Geol. (Isot. Geosci. Sect.) 66, 89–98, 1987.
21 N. Bhandari, J. Fruchter and J. Evans, Rates of production of ^{24}Na and ^{28}Mg in the atmosphere by cosmic radiation, Earth Planet. Sci. Lett. 7, 89–92, 1969.
22 K. O'Brien, Secular variation in the production of cosmogenic isotopes in the earth's atmosphere, J. Geophys. Res. 84, 423–431, 1979.
23 D. Lal, Investigations of nuclear interactions produced by cosmic rays, Ph.D. Thesis, Bombay University, 1958.
24 Manual of the ICAO Standard Atmosphere, 2nd ed., International Civil Aviatory Organization, Montreal, Que., 1964.
25 B. Lavielle, H. Sauvageon and P. Bertin, Cross-sections of Neon and Krypton isotopes produced by neutrons, Abstracts for the Workshop on Cosmogenic Nuclide Production Rates, Vienna, July 25–26, 1989, Lunar Planet. Lab., Houston, Tex., 27–28, 1989. Also see B. Lavielle, Status of charged particles and neutrons induced nuclear reactions, Abstracts for the Workshop on Cosmogenic Nuclide Production Rates, Vienna, July 25–26, 1989, Lunar Planet. Lab., Houston, Tex., pp. 25–26, 1989.
26 D. Lal and V.S. Venkatavaradan, Analysis of causes of ^{14}C variations in the atmosphere, in: Radiocarbon Variations and Absolute Chronology, pp. 549–570, I. Olsson, ed., Wiley, New York, N.Y., 1970.
27 D. Lal, Theoretically expected variations in the terestrial cosmic ray production rates of isotopes, Proc. Fermi Sch. Phys. 95th, Varenna, Ital. Acad. Sci., pp. 216–233, 1988.
28 B. Rossi, High-Energy Particles, 569 pp., Prentice-Hall, Englewood Cliffs, N.J., 1952.
29 E. Schopper, E. Lohrmann and G. Mauck, Nukleonen in der Atmosphäre, Handbuch der Physik 46/2, 372–550, 1967.
30 K. Nishiizumi, D. Elmore, X.Z. Ma and J.R. Arnold, ^{10}Be and ^{36}Cl depth profiles in an Apollo 15 drill core, Earth Planet. Sci. Lett. 70, 157–163, 1984. K. Nishiizumi, J. Klein, R. Middleton and J.R. Arnold, ^{26}Al depth profile in Apollo 15 drill core, Earth Planet. Sci. Lett. 70, 164–168, 1984.
31 J. Klein, R. Giegengack, R. Middleton and P. Sharma, Revealing histories of exposures using *in situ* produced ^{26}Al and ^{10}Be in Libyan desert glass, Radiocarbon 28, 547–555, 1988.